

Ultrahigh resolution optical coherence tomography using a superluminescent light source

Andrew M. Kowalevich, Tony Ko, Ingmar Hartl, and James G. Fujimoto

*Department of Electrical Engineering and Computer Science
and Research Laboratory of Electronics
Massachusetts Institute of Technology, Cambridge, MA 02139*

Markus Pollnau and René P. Salathé

*Institute of Applied Optics, Department of Microtechnique,
Swiss Federal Institute of Technology,
CH-1015 Lausanne, Switzerland*

Abstract: A superluminescent Ti:Al₂O₃ crystal is demonstrated as a light source for ultrahigh resolution optical coherence tomography (OCT). Single spatial mode, fiber coupled output powers of ~40 μW can be generated with 138 nm bandwidth using a 5 W frequency doubled, diode pumped laser, pumping a thin Ti:Al₂O₃ crystal. Ultrahigh resolution OCT imaging is demonstrated with 2.2 μm axial resolution in air, or 1.7 μm in tissue, with >86 dB sensitivity. This light source provides a simple and robust alternative to femtosecond lasers for ultrahigh resolution OCT imaging.

© 2002 Optical Society of America

OCIS codes: 170.4500 Optical coherence tomography; 170.3880 Medical and biological imaging; 170.3890 Medical optics instrumentation

References and links

1. D. Huang, E. A. Swanson, C. P. Lin, J. S. Schuman, W. G. Stinson, W. Chang, M. R. Hee, T. Flotte, K. Gregory, C. A. Puliafito, J. G. Fujimoto, "Optical coherence tomography," *Science* **254**, 1178-1181 (1991).
2. G. J. Tearney, M. E. Brezinski, B. E. Bouma, S. A. Boppart, C. Pitris, J. F. Southern, J. G. Fujimoto, "In vivo endoscopic optical biopsy with optical coherence tomography," *Science* **276**, 2037-2039 (1997).
3. S. A. Boppart, B. E. Bouma, C. Pitris, J. F. Southern, M. E. Brezinski, J. G. Fujimoto, "In vivo cellular optical coherence tomography imaging," *Nature Med.* **4**, 861-865 (1998).
4. B. Bouma, G. J. Tearney, S. A. Boppart, M. R. Hee, M. E. Brezinski, J. G. Fujimoto, "High-resolution optical coherence tomographic imaging using a mode-locked Ti:Al₂O₃ laser source," *Opt. Lett.* **20**, 1486-1488 (1995).
5. B. E. Bouma, G. J. Tearney, I. P. Bilinsky, B. Golubovic, "Self phase modulated Kerr-lens mode locked Cr:forsterite laser source for optical coherent tomography," *Opt. Lett.* **21**, 1839-1841 (1996).
6. I. Hartl, X. D. Li, C. Chudoba, R. Ghanta, T. Ko, J. G. Fujimoto, J. K. Ranka, R. S. Windeler, A. J. Stentz, "Ultrahigh resolution optical coherence tomography using continuum generation in an air-silica microstructure optical fiber," *Opt. Lett.* **26**, 608-610 (2001).
7. W. Drexler, U. Morgner, F. X. Kaertner, C. Pitris, S. A. Boppart, X. D. Li, E. P. Ippen, J. G. Fujimoto, "In vivo resolution optical coherence tomography," *Opt. Lett.* **24**, 1221-1223 (1999).
8. W. Drexler, U. Morgner, R. K. Ghanta, F. X. Kaertner, J. S. Schuman, J. G. Fujimoto, "Ultrahigh resolution ophthalmic optical coherence tomography," *Nature Med.* **7**, 502-507 (2001).
9. X. Clivaz, F. Marquis-Weible, R. P. Salathe, "Optical low coherence reflectometry with 1.9 μm spatial resolution," *Electron. Lett.* **28**, 1553-1554 (1994).
10. H. H. Liu, P. H. Cheng, J. Wang, "Spatially coherent white light interferometer based on a point fluorescent source," *Opt. Lett.* **18**, 678-680 (1993).
11. A. A. Anderson, R. W. Eason, L. M. B. Hickey, M. Jelinek, C. Grivas, D. S. Gill, N. A. Vainos, "Ti:sapphire planar waveguide laser grown by pulsed laser deposition," *Opt. Lett.* **22**, 1556-1558 (1997).
12. M. Pollnau, R. P. Salathe, T. Bhutta, D. P. Shepherd, R. W. Eason, "Continuous-wave broadband emitter based on a transition-metal-ion-doped waveguide," *Opt. Lett.* **26**, 283-285 (2001).

Optical Coherence Tomography (OCT) is an emerging technology for biomedical imaging.¹⁻³ Micrometer resolution, tomographic images can be generated using a Michelson interferometer with a low-coherence light source. The axial resolution in OCT imaging is governed by the coherence length of the light source and is inversely proportional to the bandwidth. Standard, ~ 10 μm axial resolution OCT imaging can be performed using superluminescent diodes (SLD) that have ~ 20 - 30 nm FWHM bandwidths centered near 800 nm. These sources are relatively inexpensive and have turn-key operation suitable for clinical use but provide limited resolutions due to their narrow bandwidths. Ultrahigh resolution OCT has been performed with broad bandwidths generated directly from femtosecond solid state lasers, as well as by using self phase modulation of femtosecond pulses in optical fibers.⁴⁻⁶ Recently, OCT imaging with axial resolutions of ~ 1 μm has been achieved using a femtosecond Ti:Al₂O₃ laser with a bandwidth of ~ 300 nm.^{7,8} Unfortunately, these systems are expensive and complex, limiting their widespread use. Fluorescence from Ti:Al₂O₃ and laser dyes have been demonstrated as sources for ultrahigh resolution low coherence reflectometry.^{9,10} Low coherence reflectometry with < 2 μm axial resolution was first demonstrated in Ti:Al₂O₃ using 4.8 μW fluorescence produced from a Ti:Al₂O₃ crystal pumped by a 20 W Argon laser. While this result demonstrated the highest resolution low coherence reflectometry achieved at that time, the output powers were not sufficient to permit imaging.

Output powers can be improved significantly using a high doping density crystal and more efficient fluorescent coupling. In this paper we demonstrate a more than one order of magnitude improvement in light source efficiency. Using 5 W cw laser pumping of a Ti:Al₂O₃ crystal, 40.3 μW of fluorescence with bandwidths of 138 nm can be coupled into a single-mode optical fiber. We achieve ultrahigh resolution OCT imaging with 2.2 μm axial resolution in air (1.7 μm in tissue) and > 86 dB sensitivity. This demonstrates that ultrahigh resolution OCT imaging may be performed using a simple light source without the need for femtosecond Ti:Al₂O₃ lasers.

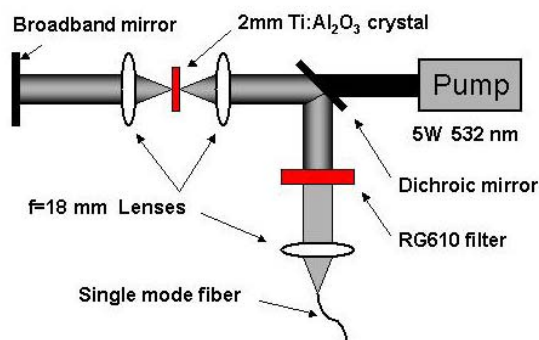


Figure 1. Experimental schematic of low coherence light source. A high doping density Ti:Al₂O₃ crystal enables pumping with a high excitation density per unit volume. A double pass pump and fluorescence collection geometry is used.

The light source is shown schematically in Figure 1. A frequency doubled Nd:Vanadate laser pumps a 2 mm thick, 1 degree wedged, Ti:Al₂O₃ crystal with an absorption coefficient of $\alpha = 7$ cm^{-1} at 532 nm. The pump light passes through a 45 degree dichroic beamsplitter which transmits 89% of pump light at 532 nm and reflects $> 99\%$ of the fluorescence between 650-950 nm. The pump is focused with an $f=18$ mm aspheric lens, AR coated for $> 99\%$ transmission from 550-1050 nm. This lens also collects and collimates the backward emitted fluorescence. A similar, $f=18$ mm aspheric lens behind the crystal collimates the fluorescence and the unabsorbed pump light. A broadband metal mirror retroreflects the collimated fluorescence as well as the remaining pump light. This double pass geometry efficiently uses

the pump power while collecting both the forward and backward emitted fluorescence. A colored glass filter (RG610) after the dichroic beam splitter removes any remaining pump light. The collimated fluorescence is focused into a 4 μm core diameter, 0.12 NA, single-mode fiber having a 633 nm cutoff wavelength using an $f=18$ mm lens with a NA that closely matches the optical fiber.

Figure 2 shows the fluorescent power coupled into the single mode fiber versus incident pump power. Figure 3 (left) shows the spectrum of the fiber-coupled fluorescence. The FWHM bandwidth was ~ 138 nm and follows the expected fluorescence spectrum of $\text{Ti:Al}_2\text{O}_3$. Both the power and spectrum were stable for periods of several hours without realignment. By cooling the crystal to -15°C , a maximum fluorescence power of $40.3 \mu\text{W}$ was achieved at 5 W of incident pump. Operating at room temperature without cooling, $34.1 \mu\text{W}$ could be generated at 5 W pump. A family of curves was obtained with the crystal cooled to different temperatures. The output power increased sublinearly at higher pump powers and this reduced efficiency was probably due to thermal effects. These results suggest that more coupled fluorescence power should be possible with better thermal control.

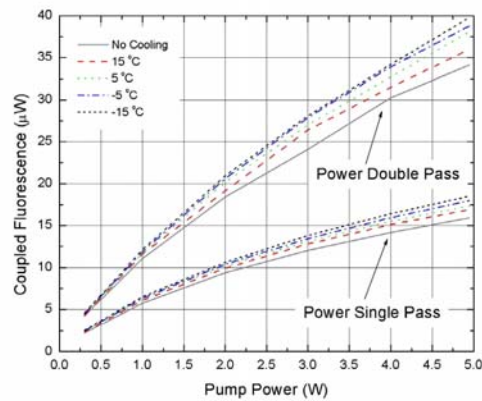


Figure 2. Output power coupled into a single mode optical fiber versus pump power. A double pass configuration approximately doubles the collected power.

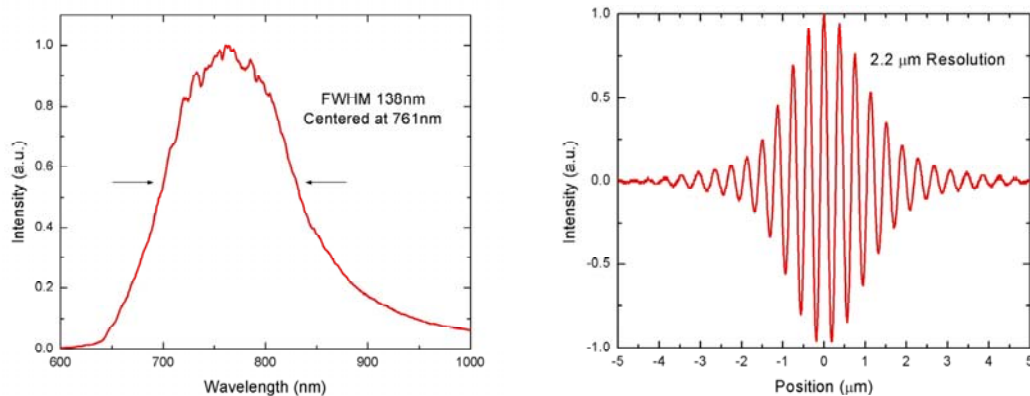


Figure 3. (left) Spectrum after coupling into a single mode optical fiber. The bandwidth is 138 nm centered at 761 nm. (right) Interference fringes from photodetector at the output of the OCT dual balanced interferometer. The axial resolution is $2.2 \mu\text{m}$ in air, corresponding to $1.7 \mu\text{m}$ in tissue.

In order to demonstrate the utility of this light source, we performed ultrahigh resolution OCT imaging. The ultrahigh resolution OCT system is shown in Figure 4. Special care was taken to maintain bandwidth and resolution. Achromatic lenses were used in the reference and sample arms and the dispersion in the arms was carefully balanced. The reference arm delay was scanned at a repetition rate of 4 Hz and a velocity of 4.4 mm/s using a galvanometer and corner cube, resulting in an interference signal Doppler frequency of 12 kHz. Figure 3 (right) shows the output of the interferometer, demonstrating a 2.2 μm axial resolution in air, or 1.7 μm in tissue. The photodetector signal was filtered with a 10 kHz bandwidth bandpass filter and log demodulated to generate OCT images. A detection sensitivity of >86 dB was achieved at an incident power of 7.3 μW on the sample. Dual balanced detection was necessary to cancel excess noise in the light source and achieve high sensitivities.

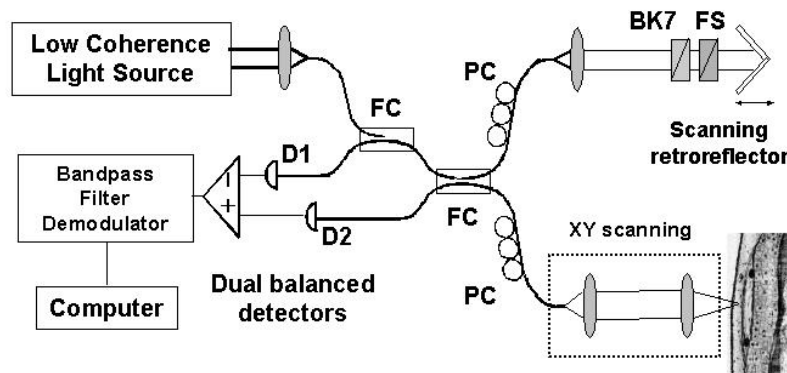


Figure 4. Schematic of ultrahigh resolution OCT system. A dual balanced interferometer was used to cancel the excess noise in the light source. Dispersion was balanced in the sample and reference arms.

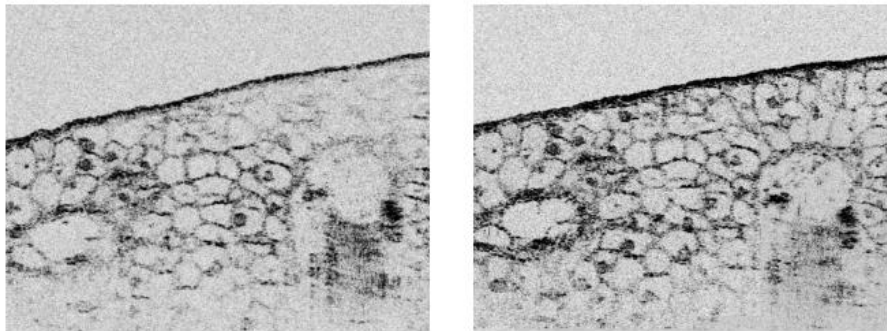


Figure 5. Ultrahigh resolution OCT imaging of African Frog (*Xenopus Laevis*) tadpole *in vivo*. (Left) Imaging was performed with <2 μm axial resolution and 5 μm transverse resolution. (Right) A composite image with extended depth of field formed by fusing 5 images with different focal depth settings.

Ultrahigh resolution OCT imaging was performed on an African frog (*Xenopus laevis*) tadpole *in vivo*. Figure 5 (left) shows an OCT image consisting of 600 transverse by 625 longitudinal pixels, covering a field of view of 600 μm by 470 μm (corrected for index of tissue) respectively. Each image consists of 600 axial scans and requires ~ 170 s to acquire.

The transverse resolution was 5 μm and the depth of field was 200 μm . An image with extended depth of field, Figure 5 (right), was constructed using C-Mode scanning.⁷ Five individual images with the focus at varying depths were fused to yield a composite image. The ultrahigh resolution OCT image shows that individual cells and nuclei are easily resolved. These results are similar to those presented in [7] and demonstrate that cellular level imaging can be performed without the need for femtosecond lasers. Although current power levels do not permit high speed imaging, ultrahigh resolution OCT imaging at low speed is possible and is sufficient for many applications including imaging materials, *in vitro* specimens, or immobile *in vivo* specimens.

Additional improvements in light source efficiency should be possible. The current system is limited by thermal effects and further reducing the temperature should improve efficiency. In addition, increasing the doping density of the $\text{Ti}:\text{Al}_2\text{O}_3$ crystal should increase the pump energy absorption density and yield a corresponding increase in fluorescence. While doping densities are limited by the onset of parasitic excited state absorption for laser applications, this fluorescence application is much less sensitive to parasitic absorption so that higher doping densities may be possible. Finally, in a bulk crystal, only a small fraction of the fluorescence is collected. The pumped volume is cylindrical; however, only fluorescence emitted within a narrow depth of field is collected. In addition, only a relatively small solid angle of the emission can be coupled into the single mode optical fiber. The use of planar or channel waveguide structures, which capture the fluorescence over a greater solid angle and integrate over a range of depths, should increase the efficiency of the fiber coupled fluorescence by more than an order of magnitude.^{11,12} These results demonstrate that fluorescent light sources can be a viable alternative to femtosecond lasers for ultrahigh resolution OCT imaging.

Acknowledgments

The authors thank Dr. Wolfgang Drexler and Pei-Lin Hsiung for helpful discussions. This research is supported in part by NIH contracts NIH-9-RO1-CA75289-04, NIH-9-RO1-EY11289-15, the AFOSR Medical Free Electron Laser Program contract F49620-01-1-0186, AFOSR contract F4920-98-1-0139, and NSF contracts ECS-0119452 and BES-0119494.

Andrew Kowalevicz is also with the Division of Engineering and Applied Sciences at Harvard University.